

Electronic Supplementary Information (ESI) For:

Neutron Diffraction Structural Study of CO₂ Binding in Mixed-Metal CPM-200 Metal-Organic Frameworks

Anthony J. Campanella,^{†a} Benjamin A. Trump,^{†b} Aeri J. Gosselin,^a Eric D. Bloch^{*ac} and Craig M. Brown^{*bd}

*edb@udel.edu

*craig.brown@nist.gov

^aDepartment of Chemistry & Biochemistry, University of Delaware, Newark, DE 19716, USA. E-mail: edb@udel.edu, craig.brown@nist.gov.

^bCenter for Neutron Research, National Institute of Standards and Technology, Gaithersburg, MD 20899, USA.

^cCenter for Neutron Science, Department of Chemical and Biomolecular Engineering, University of Delaware, Newark, DE 19716, USA.

^dDepartment of Chemical and Biomolecular Engineering, University of Delaware, Newark, DE 19716, USA.

[†]These authors contributed equally and are joint first authors.

List of Contents

Detailed Experimental Procedures	S3
Neutron Diffraction Analysis	S4
Neutron Powder Diffraction	S5
Gas Adsorption Isotherms	S10
Surface Area Plots	S13
References	S15

Experimental Section

General Considerations. All reagents were obtained from commercial vendors and used without further purification. All adsorption measurements were obtained on a Micromeritics 3Flex.

Synthesis of 3,3'-5,5'-azobenzenetetracarboxylic acid (H₄ABTC)

Given the relatively low proton content of this ligand, deuteration—the main advantage of which would be better quality data with more reflections out to higher angles and reduced our errors on the refinements, was not necessary. Given the inherent disorder in these materials (mixed metal sites and missing linkers) deuteration would not have greatly improved diffraction results.

The following procedure was adapted from previous literature.¹ Generally, 5-nitro-1,3-benzenedicarboxylic acid (2.1 g, 0.01 mol), zinc (1.3 g, 0.015 mol), and sodium hydroxide (0.8g, 0.02 mol) were added to a 250 mL RBF. Ethanol (50 mL) and DI water (20 mL) were added to the reaction flask. The mixture was heated to reflux for 12 hours. Upon cooling, a yellow solid precipitated out of solution and was separated from the mother liquor via vacuum filtration. The yellow solid was collected and dissolved in a 1M solution of sodium hydroxide (50 mL). Any insoluble solid was separated via filtration. The filtrate was then acidified with concentrated HCL until the solution reached a pH = ~3. Orange product was collected and dried via vacuum filtration.

Synthesis of VMg₂-PCN-250

This material was made according to the literature procedure.² Activated sample was obtained via the following method. As synthesized material was washed with fresh methanol 3x with solvent being replaced with fresh methanol every 24 hours. Methanol was then removed from the sample vial. Vial was placed in a vacuum tube and connected to a Teflon pump to remove excess methanol. Activated material was obtained by heating at 120 °C for 4 days.

Synthesis of InMg₂-PCN-250

The following procedure was adapted from previous literature.² InCl₃ (0.442 g, 2 mmol), Mg(OAc)₂ (1.72 g, 8 mmol), and H₄ABTC (0.712 g, 1.9 mmol) were added into a 100 mL VWR jar. Dimethylacetamide (DMA) (80 g), DI water (16 g), and conc. HCl (2.4 g) were added to the jar. The reaction mixture was then heated at 100 °C for 2 days. Activated sample was obtained via the following method. As synthesized material was washed with fresh DMA 3x with solvent being replaced with fresh methanol every 24 hours. DMA washed material was then solvent exchanged with fresh methanol, solvent was replaced every 24 hours 3 times. Methanol was then removed from the sample vial. Vial was placed in a vacuum tube and connected to a Teflon pump to remove excess methanol. Activated material was obtained by heating at 120 °C for 4 days.

Synthesis of Fe₂Mg-PCN-250

The following procedure was adapted from previous literature.² FeCl₃ (0.54 g, 3.3 mmol), Mg(OAc)₂ (1.72 g, 8 mmol), and H₄ABTC (0.712 g, 1.9 mmol) were added into a 100 mL VWR jar. Diethylformamide (DEF) (80 g), DI water (16 g), and conc. HCl (2.4 g) were added to the jar. The reaction mixture was then heated at 100 °C for 5 days. Activated sample was obtained via the following method. As synthesized material was washed with fresh DEF 3x with solvent being replaced with fresh methanol every 24 hours. DEF washed

material was then solvent exchanged with fresh methanol, solvent was replaced every 24 hours 3 times. Methanol was then removed from the sample vial. The vial was placed in a vacuum tube and connected to a Teflon pump to remove excess methanol. Activated material was obtained by heating at 100 °C under dynamic vacuum for 16 hours and then heated to 120 °C for 30 hours.

Neutron Diffraction Analysis

Neutron powder diffraction measurements were performed on 0.360 g $\text{In}_{0.90}\text{Mg}_{2.10}\text{O}(\text{ABTC})_{1.26}$ (InMg_2), 0.181 g $\text{V}_{0.88}\text{Mg}_{2.21}\text{O}(\text{ABTC})_{1.25}(\text{H}_2\text{O})_{2.46}$ (VMg_2), ~0.3 g $\text{Fe}_{2.04}\text{Mg}_{0.96}\text{O}(\text{ABTC})_{1.5}(\text{H}_2\text{O})_{1.2}$, and 1.362 g $\text{Fe}_{2.09}\text{Mg}_{0.91}\text{O}(\text{ABTC})_{1.5}(\text{H}_2\text{O})_{1.2}$ (Fe_2Mg), where ABTC = 3,3',5,5'-azobenzene tetracarboxylic acid, at the National Institute of Standards and Technology Center for Neutron Research (NCNR) using the high-resolution neutron powder diffractometer, BT1. Data was collected using a Ge(311) monochromator with an in-pile 60' collimator, corresponding to a neutron wavelength of 2.0775 Å. Methanol exchanged samples were activated at 120 °C for 4-8 days depending on sample size. Immediately after activation samples were loaded into vanadium samples cans, in a He environment glovebox, and sealed with an indium o-ring onto a copper heating block containing a valved outlet for gas loading. The assembly was then mounted onto a bottom-loaded closed cycle refrigerator (CCR) and connected to a gas manifold of known volume. Initial diffraction measurements were conducted at base temperature for each CCR on activated materials. Samples were heated to at least 220 K for CO_2 gas doses, with full adsorption verified barometrically before cooling to base temperatures to avoid condensation of the vapor phase prior to each diffraction measurement. Refinements were conducted using Topas Academic.³

Disclaimer: Certain commercial equipment, instruments, materials, or software are identified in this paper to foster understanding. Such identification does not imply recommendation or endorsement by the National Institute of Standards and Technology, nor does it imply that the materials or equipment identified are necessarily the best available for the purpose.

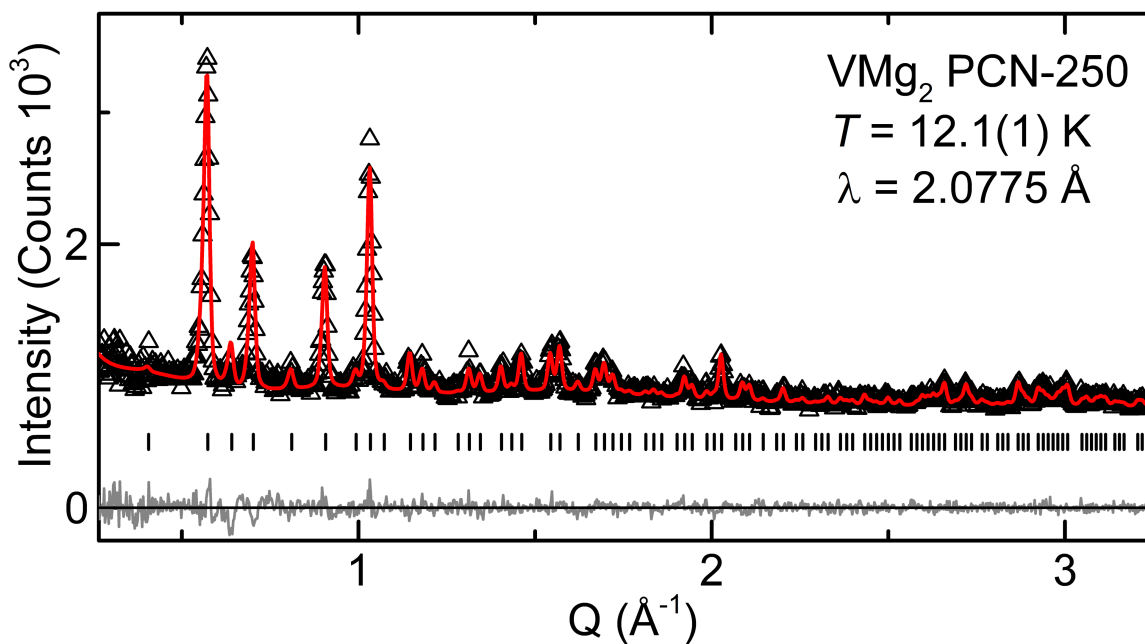


Figure S1. Rietveld refinement of neutron powder diffraction data for $V_{0.88(4)}Mg_{2.21(11)}O(ABTC)_{1.25(5)}(H_2O)_{2.46(18)}$. Data shown as black triangles, fit displayed in red, and difference curve shown in gray. Fit statistics were $R_{exp} = 3.97$ %, $R_{wp} = 3.72$ %, $R_p = 3.22$ %, $GoF = 0.937$. Symbols are commensurate with experimental error.

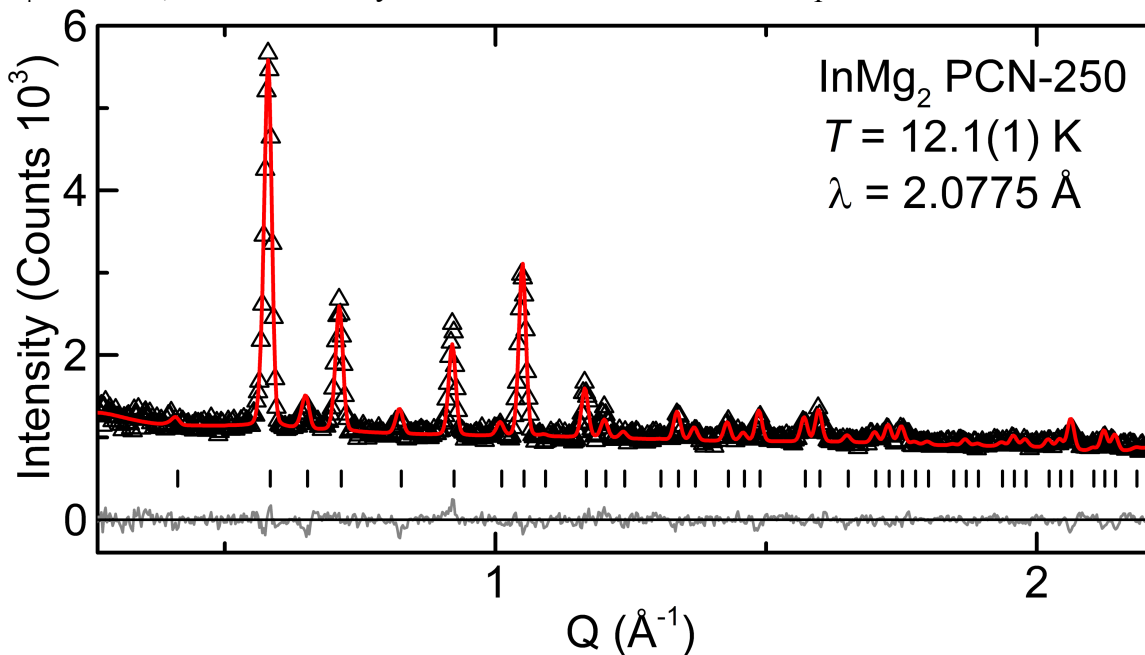


Figure S2. Rietveld refinement of neutron powder diffraction data for $In_{0.90(5)}Mg_{2.10(11)}O(ABTC)_{1.26(6)}$. Data shown as black triangles, fit displayed in red, and difference curve shown in gray. Fit statistics were $R_{exp} = 4.00$ %, $R_{wp} = 4.66$ %, $R_p = 3.73$ %, $GoF = 1.16$. Symbols are commensurate with experimental error.

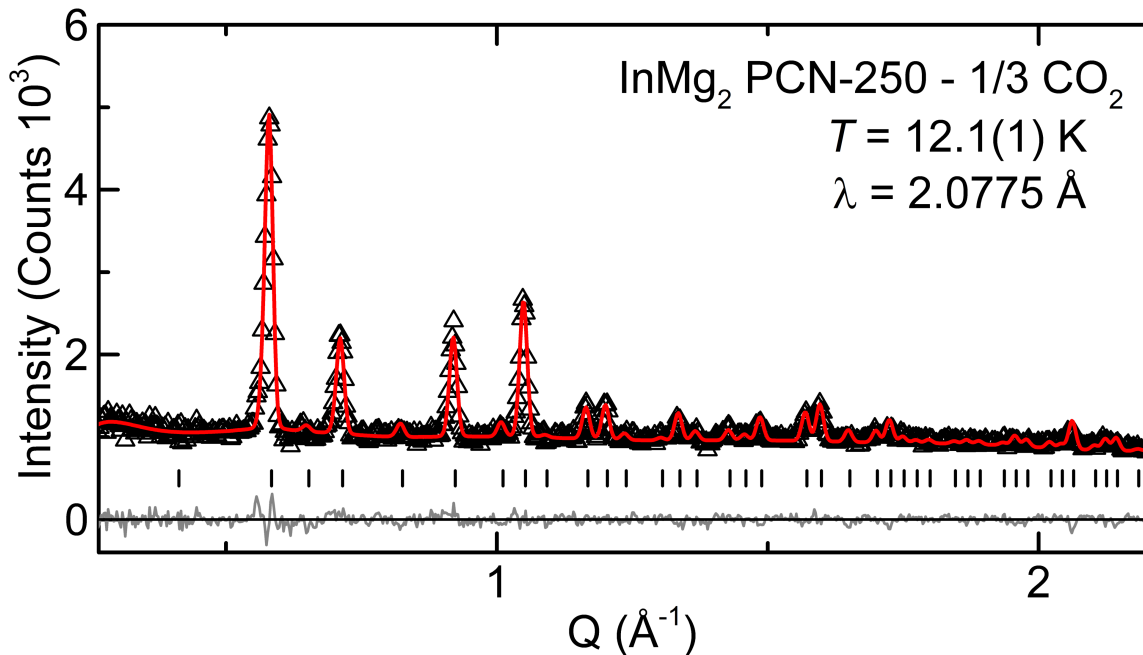


Figure S3. Rietveld refinement of neutron powder diffraction data for $\text{In}_{0.90(5)}\text{Mg}_{2.10(11)}\text{O}(\text{ABTC})_{1.26(6)}(\text{CO}_2)_{1.04(12)}$ ($\sim 1/3$ eq. per metal of CO_2). Data shown as black triangles, fit shown in red, and difference curve displayed in gray. Fit statistics were $R_{\text{exp}} = 4.09\%$, $R_{\text{wp}} = 4.54\%$, $R_p = 3.75\%$, $\text{GoF} = 1.08$. Symbols are commensurate with experimental error.

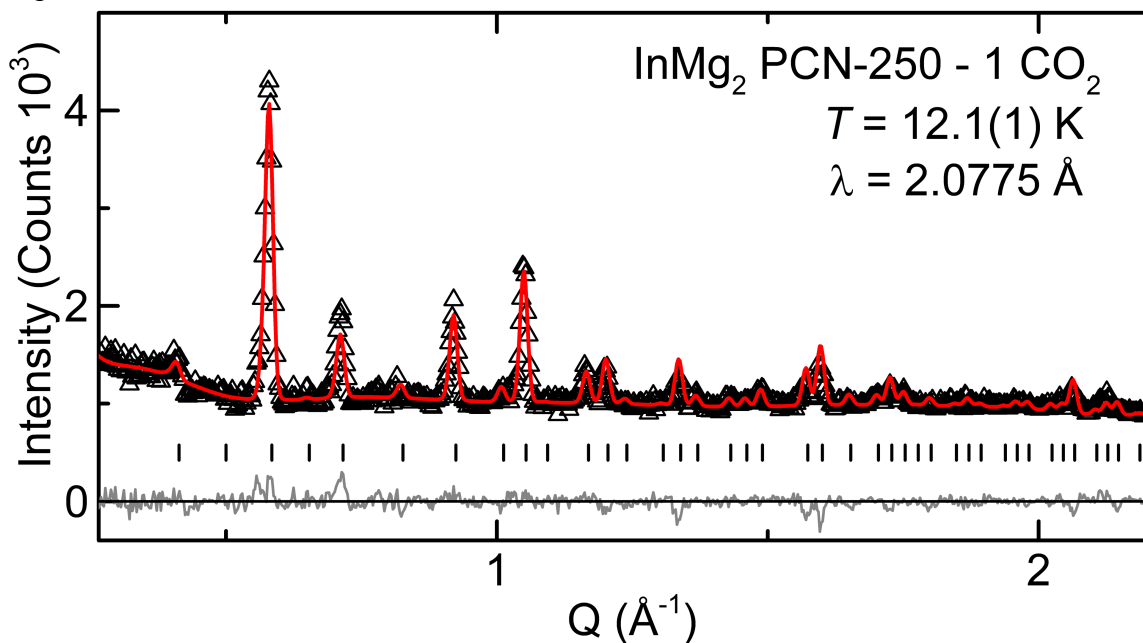


Figure S4. Rietveld refinement of neutron powder diffraction data for $\text{In}_{0.90(5)}\text{Mg}_{2.10(11)}\text{O}(\text{ABTC})_{1.26(6)}(\text{CO}_2)_{3.30(7)}$ (~ 1 eq. per metal of CO_2). Data shown as black triangles, fit shown in red, and difference curve displayed in gray. Fit statistics were $R_{\text{exp}} = 4.04\%$, $R_{\text{wp}} = 4.83\%$, $R_p = 3.94\%$, $\text{GoF} = 1.20$. Symbols are commensurate with experimental error.

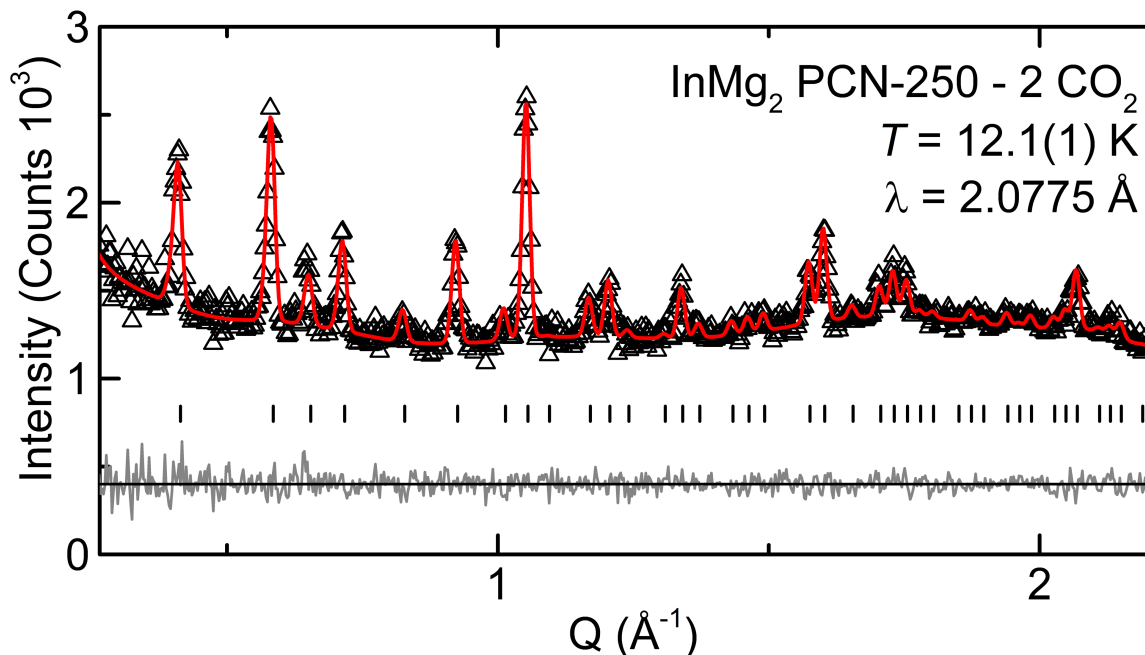


Figure S5. Rietveld refinement of neutron powder diffraction data for $\text{In}_{0.90(5)}\text{Mg}_{2.10(11)}\text{O}(\text{ABTC})_{1.26(6)}(\text{CO}_2)_{5.78(5)}$ (~ 2 eq. per metal of CO_2). Data shown as black triangles, fit displayed in red, and difference curve shown in gray. Fit statistics were $R_{\text{exp}} = 3.58\%$, $R_{\text{wp}} = 3.22\%$, $R_p = 2.69\%$, $\text{GoF} = 0.900$. Symbols are commensurate with experimental error.

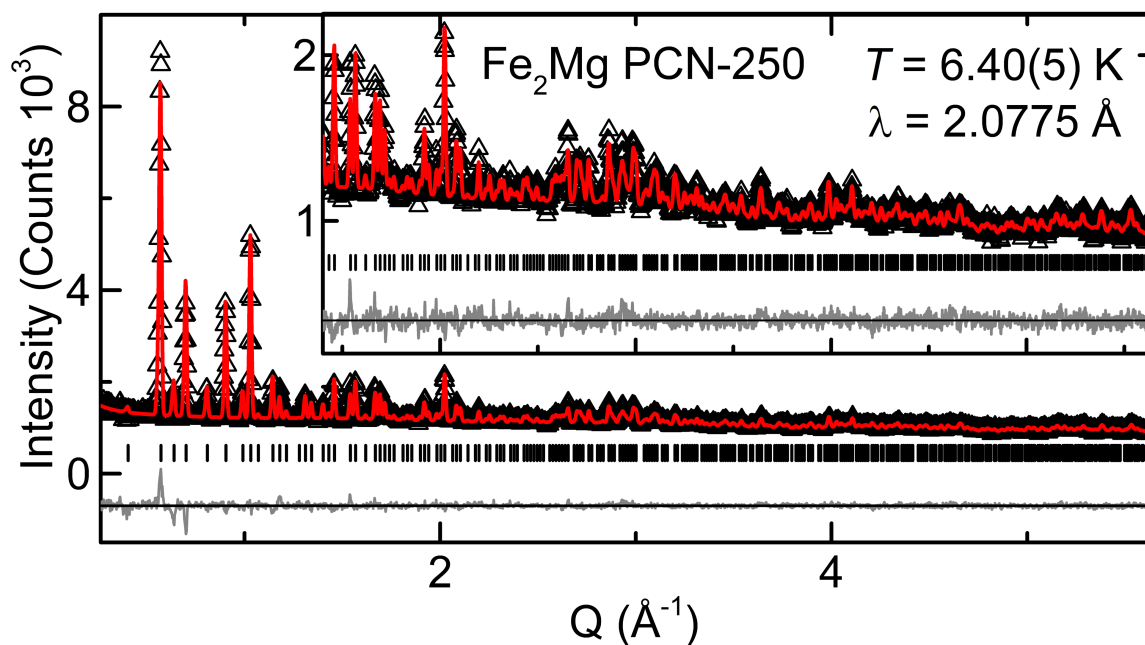


Figure S6. Rietveld refinement of neutron powder diffraction data for $\text{Fe}_{2.04(10)}\text{Mg}_{0.96(5)}\text{O}(\text{ABTC})_{1.5}(\text{H}_2\text{O})_{1.17(13)}$. Data shown as black triangles, fit shown in red, and difference curve displayed in gray. Fit statistics were $R_{\text{exp}} = 3.00\%$, $R_{\text{wp}} = 3.29\%$, $R_p = 2.77\%$, $\text{GoF} = 1.10$. Symbols are commensurate with experimental error.

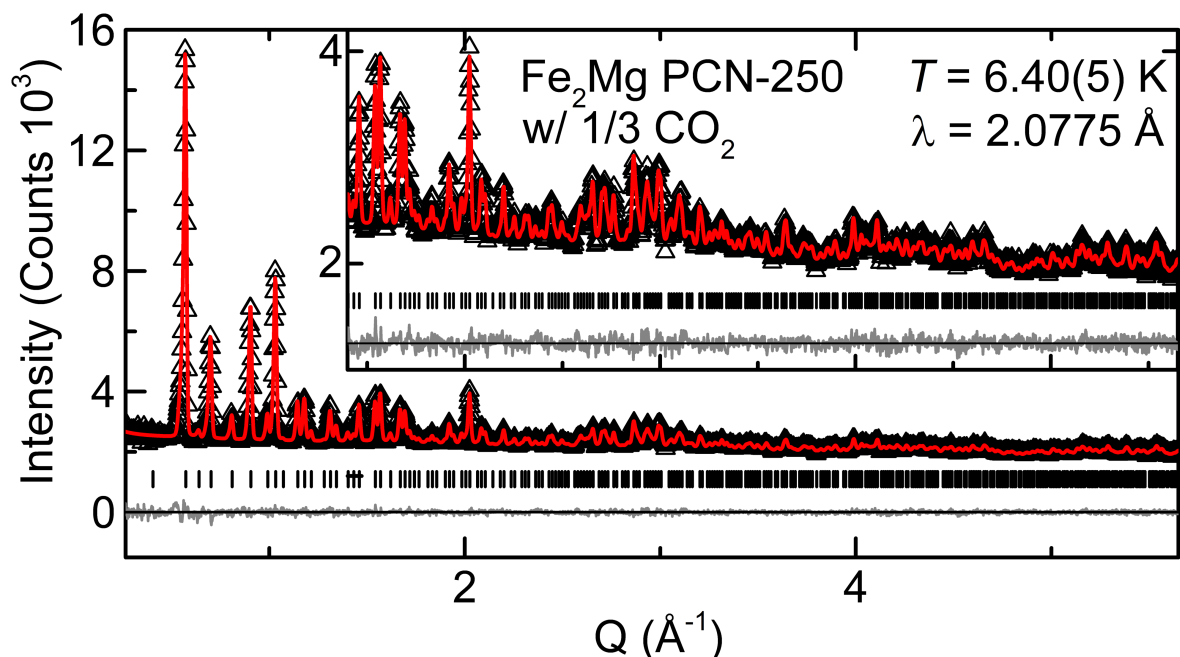


Figure S7. Rietveld refinement of neutron powder diffraction data for $\text{Fe}_{2.09(10)}\text{Mg}_{0.091(5)}\text{O}(\text{ABTC})_{1.5}(\text{H}_2\text{O})_{1.17(13)}(\text{CO}_2)_{1.28(3)}$ ($\sim 1/3$ eq. per metal of CO_2). Data shown as black triangles, fit shown in red, and difference curve displayed in gray. Fit statistics were $R_{\text{exp}} = 2.12\%$, $R_{\text{wp}} = 2.16\%$, $R_{\text{p}} = 1.82\%$, $\text{GoF} = 1.02$. Symbols are commensurate with experimental error.

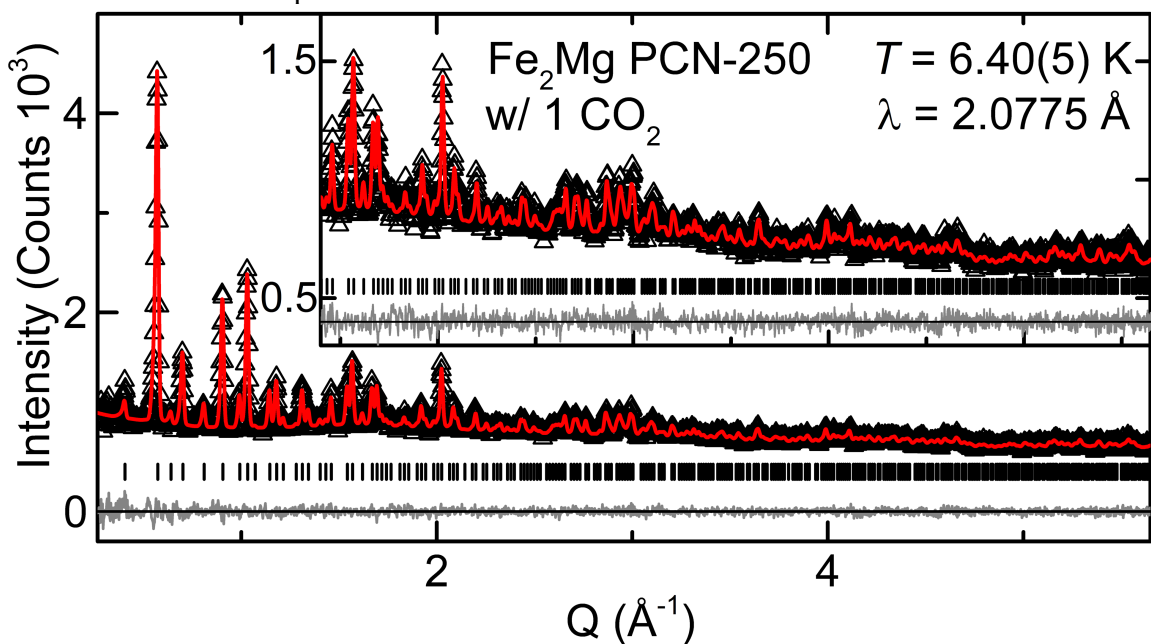


Figure S8. Rietveld refinement of neutron powder diffraction data for $\text{Fe}_{2.09(10)}\text{Mg}_{0.091(5)}\text{O}(\text{ABTC})_{1.5}(\text{H}_2\text{O})_{1.17(13)}(\text{CO}_2)_{3.25(4)}$ (~ 1 eq. per metal of CO_2). Data shown as black triangles, fit shown in red, and difference curve displayed in gray. Fit statistics were $R_{\text{exp}} = 3.61\%$, $R_{\text{wp}} = 3.27\%$, $R_{\text{p}} = 2.77\%$, $\text{GoF} = 0.907$. Symbols are commensurate with experimental error.

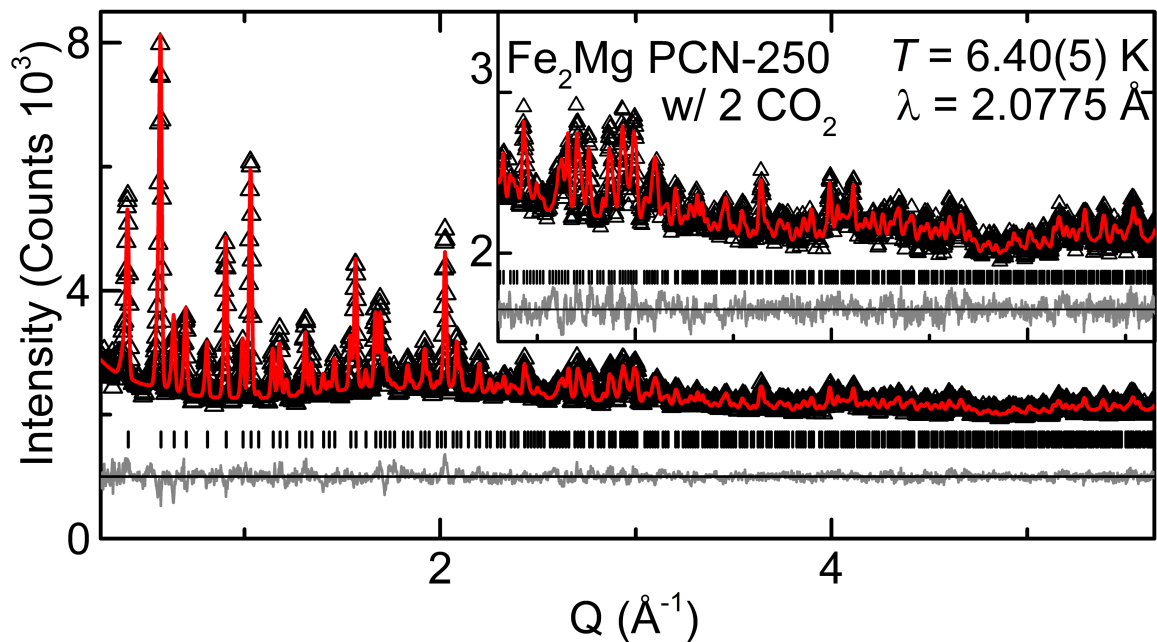


Figure S9. Rietveld refinement of neutron powder diffraction data for $\text{Fe}_{2.09(10)}\text{Mg}_{0.091(5)}\text{O}(\text{ABTC})_{1.5}(\text{H}_2\text{O})_{1.17(13)}(\text{CO}_2)_{5.87(5)}$ (~ 2 eq. per metal of CO_2). Data shown as black triangles, fit shown in red, and difference displayed curve in gray. Fit statistics were $R_{\text{exp}} = 2.12\%$, $R_{\text{wp}} = 2.45\%$, $R_{\text{p}} = 2.11\%$, $\text{GoF} = 1.16$. Symbols are commensurate with experimental error.

Gas Adsorption Isotherms

Fitting of Isotherms

The adsorption isotherms were fit with single or dual-site Langmuir-Freundlich model (Eqn. 1), where n is the absolute amount adsorbed in mmol/g, P is the pressure in bar, $q_{\text{sat},i}$ is the saturation capacity in mmol/g, b_i is the Langmuir parameter in bar^{-1} , and v_i is the Freundlich parameter for site i . The parameters used to fit the adsorption isotherms can be found in Tables S1-S3. Plots of the adsorption isotherms along with their fits are presented in Figures S10-S12.

$$\text{Equation 1.} \quad n = \frac{q_{\text{sat},1} b_1 P^{v_1}}{1 + b_1 P^{v_1}} + \frac{q_{\text{sat},2} b_2 P^{v_2}}{1 + b_2 P^{v_2}}$$

The isosteric heats of adsorption, $-Q_{\text{st}}$, were calculated through the use of the Clausius-Clapeyron equation (Eqn 2) for each gas using single-site Langmuir-Freundlich fits for each material at 298 K, 308 K, and 318 K. P is the pressure, n is the amount adsorbed, T is the temperature, R is the universal gas constant, and C is a constant. Based on plots of $(\ln P)_n$ as a function of $1/T$ the isosteric heat adsorption was obtained by the slope.

$$\text{Equation 2.} \quad \ln P = -\frac{Q_{\text{st}}}{R} \left(\frac{1}{T} \right) + C$$

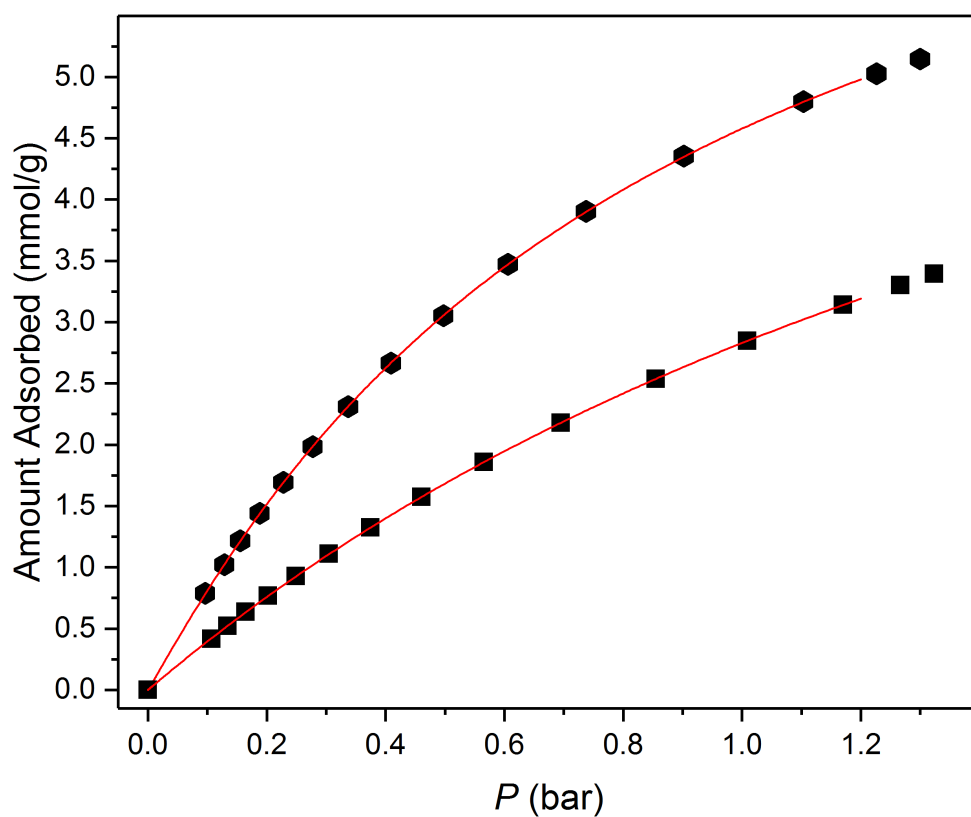


Figure S10. CO₂ adsorption in VMg₂-PCN-250 at 273 K (hexagons) and 298 K (squares). The red lines are the respective single-site Langmuir-Freundlich fits using the parameters in Table S1.

Table S1

	273 K	298 K
$q_{\text{sat},1}$	8.594 ± 0.038	8.749 ± 0.086
b_1	1.139 ± 0.011	0.478 ± 0.007
v_1	1.039 ± 0.003	1.005 ± 0.003

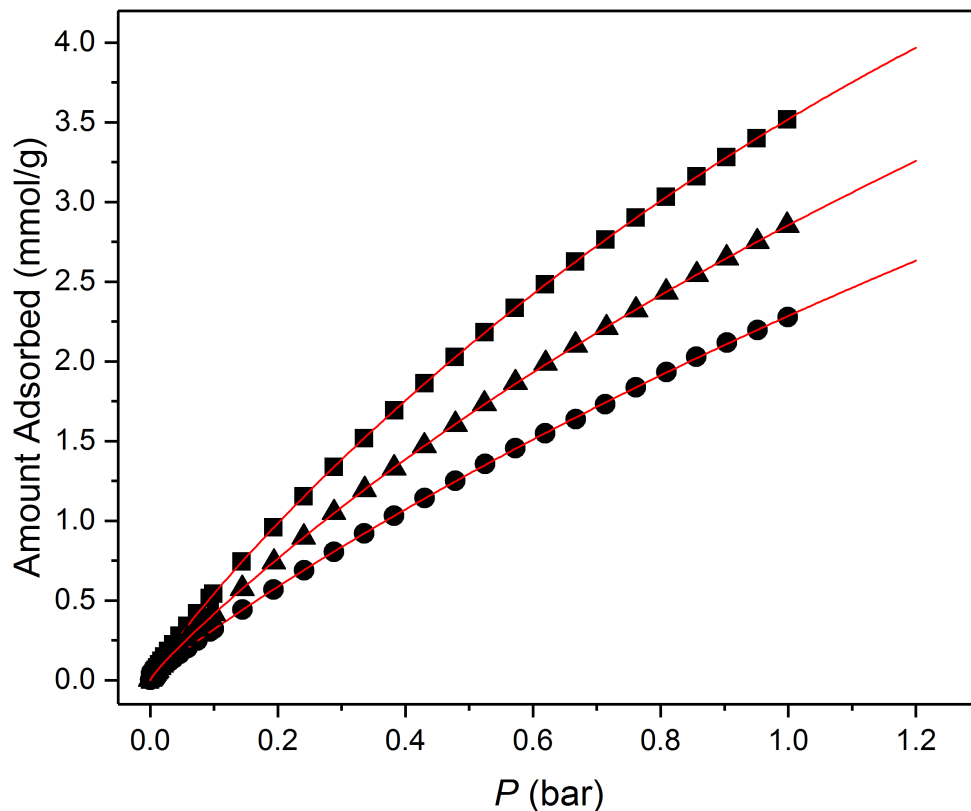


Figure S11. CO₂ adsorption in InMg₂-PCN-250 at 298 K (squares), 308 K (triangles), and 318 K (circles). The red lines are the respective single-site Langmuir-Freundlich fits using the parameters in Table S2.

Table S2

	298 K	308 K	318 K
$q_{\text{sat},1}$	6.645 ± 1.523	0.603 ± 0.707	14.304 ± 1.565
b_1	0.479 ± 0.008	1.819 ± 1.615	0.188 ± 0.024
v_1	1.327 ± 0.113	1.525 ± 0.401	0.941 ± 0.016
$q_{\text{sat},2}$	2.226 ± 1.135	26.686 ± 9.849	0.018 ± 0.007
b_2	1.564 ± 0.567	0.102 ± 0.032	1111.208 ± 7487.233
v_2	0.859 ± 0.018	0.843 ± 0.033	1.103 ± 0.997

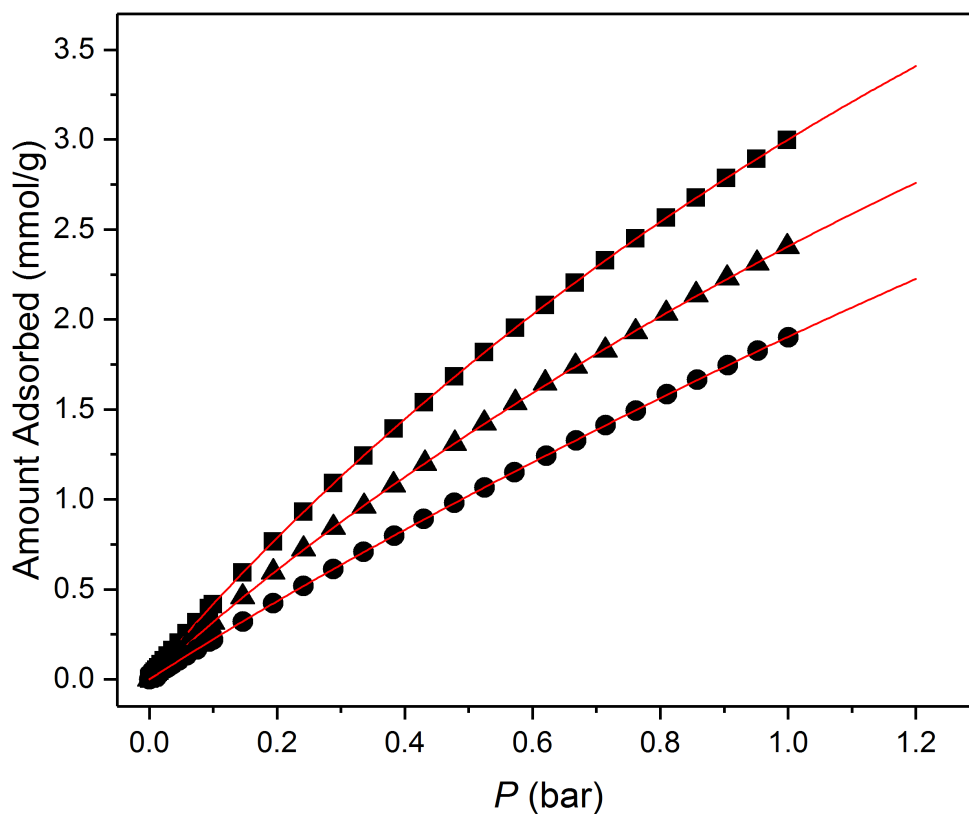


Figure S12. CO₂ adsorption in Fe₂Mg-PCN-250 at 298 K (squares), 308 K (triangles), and 318 K (circles). The red lines are the respective single-site Langmuir-Freundlich fits using the parameters in Table S3.

Table S3

	298 K	308 K	318 K
$q_{\text{sat},1}$	9.489 ± 0.629	5.831 ± 7.224	3.037 ± 15.879
b_1	0.417 ± 0.018	0.347 ± 0.153	0.226 ± 0.156
v_1	1.081 ± 0.039	1.416 ± 0.865	1.934 ± 2.971
$q_{\text{sat},2}$	0.245 ± 0.138	1.304 ± 2.496	3.134 ± 13.331
b_2	5.725 ± 2.250	2.263 ± 2.499	0.750 ± 3.017
v_2	0.916 ± 0.025	0.999 ± 0.084	1.009 ± 0.044

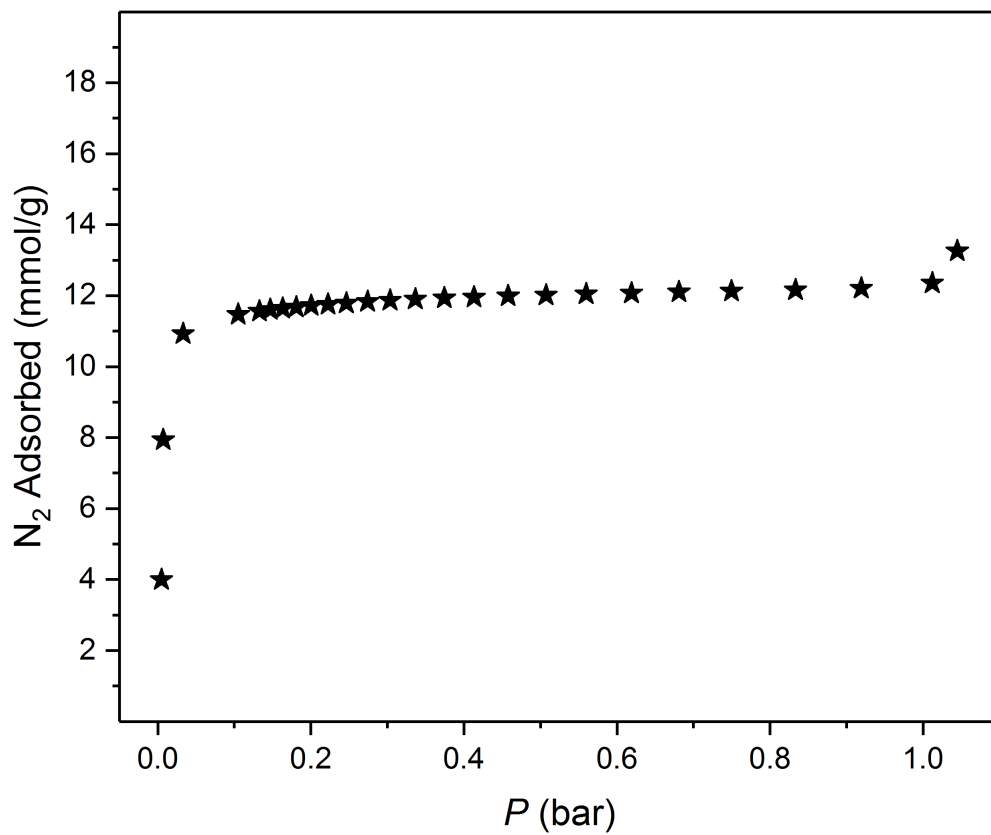


Figure S13. N₂ adsorption in VMg₂-PCN-250 at 77 K.

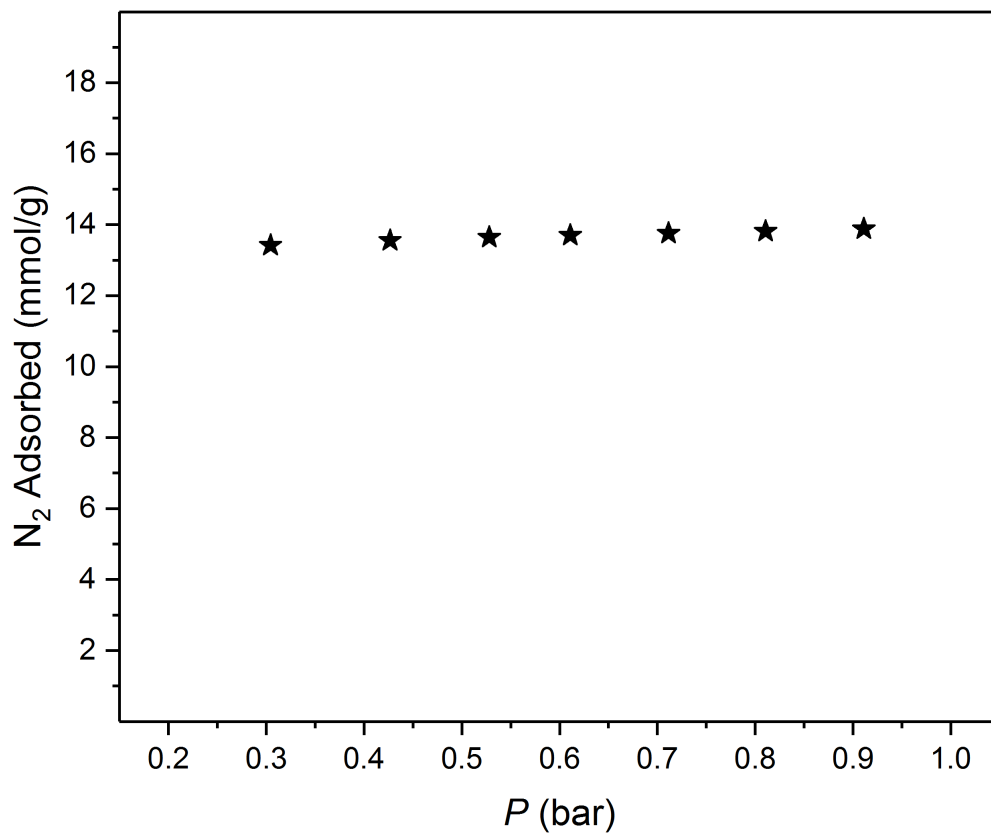


Figure S14. N₂ adsorption in InMg₂-PCN-250 at 77 K.

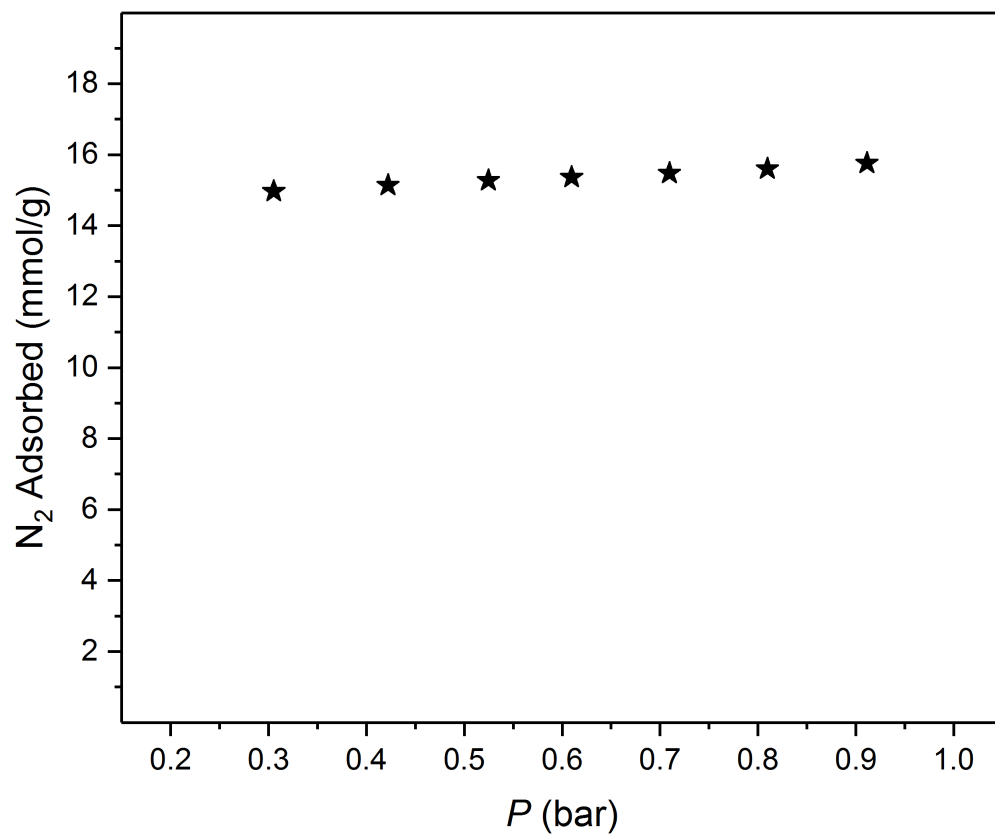


Figure S15. N₂ adsorption in Fe₂Mg-PCN-250 at 77 K.

References

- 1 S. Wang, R. C. Advincula, *Org. Lett.* 2001, **3**, 3831-3834
- 2 Q-G. Zhai, X. Bu, C. Mao, X. Zhao, P. Feng, *J. Am. Chem. Soc.* 2016, **138**, 2524-2527
- 3 A. Coelho, A. Topas Academic V6. *Coelho Softw.* 2017.